On Mitigating Wind Energy Variability with Storage

Vijay Arya, Partha Dutta, Shivkumar Kalyanaraman
IBM–Research India
{vijay.arya, parthdut, shivkumar-k}@in.ibm.com

***Abstract*—Reducing fluctuations and mitigating the variability of wind energy is essential for its integration in grids, electricity markets, microgrids, and distributed generation settings. In this work, we present a storage-based wind power smoothing system that uses novel optimization algorithms to reduce the variability of wind energy. The system considers forecasted and actual energy generated, battery size, and energy prices and determines export rates that have low variability and maximize either the energy exported or revenue earned. Our optimization algorithms are novel as they model an equivalent relaxed buffer system that uses only linear constraints and allows the computation of optimal smoothing solutions in an efficient manner. This enables the system to be used in an online manner in real time as well as in planning and operations. The smoothing system and the mathematical models and programs used in optimization are presented along with preliminary simulation results that demonstrate the need and effectiveness of the system with the help of real wind energy data. Finally, we compare wind smoothing to video smoothing and point out the important similarities and differences.**

I. Introduction

Wind is a major source of renewable energy that is being used all over the world today. Wind power is being used in grid and micro-grid settings for a number of different applications including powering residential customers, power-hungry data centers [1], [2], and base stations in mobile wireless networks [3], [4]. According to the global wind energy council, by the end of 2009, the cumulative installed wind power capacity worldwide was about 160GW. In US alone, the installed capacity is expected to grow at a rate of 10-15GW per year reaching about 300GW by 2030 [5]. In US and EU, the governments have also crafted green policies that mandate operators to source a fraction of their supplied energy from renewable sources thereby reducing CO_2 emissions.

However the inherent variability and uncertainty of wind energy makes it non-dispatchable and hard to integrate into power grids. Wind is highly variable and intermittent resulting in power that varies over multiple time scales. Moreover the generated power also depends on factors such as weather, temperature, height of the mill, and size of turbine blades, all of which contribute to compounding its variability. Today in most grids worldwide, wind power penetration levels are quite low (generally below 20%) and most of the baseload, load-following, and peaker generation requirements are met from dispatchable sources of power such as coal, nuclear, hydro, or gas/oil plants. Consequently, grids can absorb fluctuations arising out of a small amount of wind power by ramping a few dispatchable generators. Some of the variability also balances out when wind power is sourced from geographically diverse locations. However as wind becomes a larger and significant portion of the generation portfolio, mitigating its variability will become increasingly important to ensure grid reliability and sustainability. Large penetrations of wind power can increase the load-following variability faced by non-wind generation and negatively impact system ramping requirements. This can lead to a number of problems such as higher costs of cycling power plants, uneconomic dispatch of generation, higher reserve requirements, higher energy prices, and blackouts [6]–[10].

Variability in generation also impacts participation in electricity markets. Merchant producers and retailers of power interact using wholesale electricity markets such as day-ahead (DA) and real-time (RT) markets. After markets close, participants are committed to supplying or consuming energy at location-based marginal prices for an upcoming time interval. Conventional generation sources are penalized if they deviate from their commitments. Due to the variability and uncertainity of wind power, existing approaches lack a proper mechanism for wind power producers to participate in DA markets. Currently wind power is settled at RT price or sold on long-term power purchase agreements. Additionally, if the grid load is low and generation is high (e.g. at night), operators may not be able to sell power and resources are wasted. Thus existing approaches are not optimal for wind farm operators as they are unable to get the maximum economic gain for the power they generate. Accordingly, there is a need to mitigate the variability of wind energy to integrate its generators into electricity markets [11].

In this work, we present an optimization-based wind power smoothing system [12] (Fig 1), which uses forecasting and storage technologies to mitigate the variability of wind energy and facilitate its integration into grids and electricity markets. The system considers the forecasted and actual energy generated, energy storage size, and energy prices if available and determines a uniform export rate that maximizes either the total energy exported or revenue earned. It considers penalty costs for deviations from an existing export rate and determines a piece-wise linear export curve that has low variability while minimizing any wastage of energy. Using a day-ahead wind energy forecast, the system can compute a smooth export curve that can be used to plan a day-ahead energy delivery schedule. The system uses optimization that is computationally efficient so that it can be extended to work in an online manner wherein it solves the optimization using successive forecasts available at each time step to determine the export rate for the next time step.

The proposed system enables wind power generators to get better economic benefits for the power they generate and helps independent power system operators (ISOs) to integrate more wind generation into their system in a reliable and sustainable manner. In particular, the key contributions of our work are:

1. A wind power smoothing system is presented that uses power forecast and storage to determine an energy export curve that minimizes variability and maximizes energy output. Additionally, given variable energy prices, the system maximizes total revenue. The system can be used to plan ahead or invoked continuously for real-time operations. The system can be used to export energy to the grid or to captive loads in microgrid environments.
2. We develop novel mathematical programming based optimization formulations for buffer-based smoothing problem, which are computationally efficient and can be solved in polynomial time. The buffer model considers overflow as well as storage losses due to charging and discharging operations.
3. The buffer-based smoothing problem is studied using cumulative input and output curves which sheds new light on the smoothing problem. Our optimization formulations model an equivalent relaxed buffer based system using only linear constraints and still yield smoothing solutions that are optimal in terms of formulations that model the full functionality of a buffer using integer constraints.
4. We present preliminary experimental results using real wind energy data that demonstrate the operational impacts of injecting wind energy into a power system and the results of the proposed optimization algorithms.
5. We draw parallels between wind and video smoothing and show that some of the wind smoothing problems can be regarded as variants of video smoothing problems. Our work broadens the applicability of networking research to other domains and helps build synergies between networking and smart grids.

In the balance of the paper, section II compares related work followed by section III which presents the mathematical model of a buffer-based smoothing system. Section IV presents the main optimization formulations and results for the system that maximizes the energy exported. Section V presents the formulation that incorporates energy prices to maximize revenue. Section VI presents experimental results. Section VII draws parallels between variants of wind and video smoothing problems and we conclude in section VIII with directions for future work.

II. Related Work

Wind power exhibits significant variability due to intermittent and variable wind speeds. However wind power forecasting is a well-established domain due to its importance in integrating wind energy into grids [13]. Several forecasting systems that forecast at different time scales are utilized all over the world [14], [15]. Forecasts are available either as point forecasts, which give the most likely prediction for a future time period, or more sophisticated probabilistic forecasts that include the probability density functions as well [13]. Most of the wind power forecasts are currently given as point forecasts and in this work we essentially assume the availability of short-term point forecasts (up to a day or two).

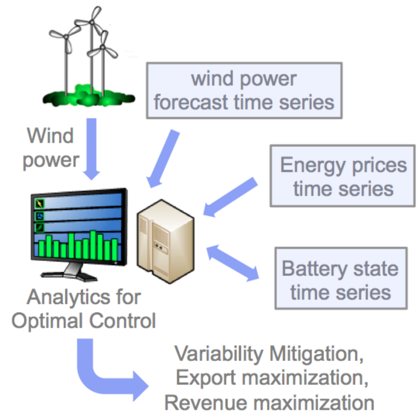

Fig. 1. A storage-based wind power smoothing system that employs novel computationally efficient optimization algorithms. The system can be used to reduce the variability of wind energy and maximize the energy exported or revenue earned.

A number of grid storage technologies are being considered for different smart grid applications including integrating renewable power sources such as wind [16]. These include CAES (compressed air energy storage), pumped hydro, flywheels, supercapacitors, and battery technologies such as sodium-sulphur or lithium-ion. The choice of storage technology depends on application requirements as well as storage characteristics such as size, weight, cost, lifetime, efficiency, and per-cycle costs. Current costs of energy storage are significant and therefore storage needs to be used optimally in order to offer competitive energy prices in the market and integrate wind power in a sustainable manner. Our work is independent of the storage technology and assumes the availability of an energy storage system of a certain capacity and models the losses due to charging/discharging operations.

Several papers have proposed storage-based solutions to efficiently dispatch wind power [17]–[20]. In [17], authors study different storage technologies in the context of wind power. In [18], the authors propose a battery storage system for smoothing power from a wind farm based on a feedback-based control framework. However, unlike our work the authors do not explicitly model the penalty for change in the export rate nor maximize the total energy exported. The authors also do not consider electricity prices (forecasted or actual). Finally, authors consider only hour-ahead wind power prediction for smoothing, whereas our work can consider longer horizons as well. In [19], the authors study the battery capacity required to maximize the economic benefit of a wind farm given energy prices and battery capital costs. However unlike our work, the authors do not consider time-varying energy prices and the penalty due to variation in export. In [20], authors consider a hybrid system with storage and a braking resistor to improve the power quality and stability of a wind farm. None of the prior works considers the design of computationally efficient mathematical programs for smoothing wind energy which is one of the focus of our work. We model the buffer using novel linear constraints which enables the computation of fast smoothing solutions.

The problem of smoothing wind power has similarities with the work on video smoothing [21]–[26]. However there are differences as well and existing solutions cannot be used readily. In a streaming system, the server needs to determine streaming rates that allow the receiver to play the video according to a specific playback curve without overflowing or starving the receiver buffer. On the other hand in a wind smoothing system, given a forecasted generation curve, the smoothing system needs to determine export rates that minimize buffer overflow/starvation and variability. We highlight the important similarities and differences between wind smoothing and video smoothing problems in section VII.

III. Mathematical Models: generation, export, storage, and wastage

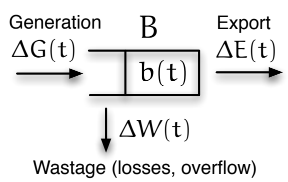

Fig. 2. The buffer model for a battery or energy storage of capacity B.

In order to motivate our approach in the subsequent sections, we now describe the mathematical model of a system that uses a point forecast and a storage of finite capacity to export wind energy (for e.g. to the grid). We consider a discrete time system that determines the amount of energy to be exported at the end of each time step given the forecast for the next n time steps. The novelty of the modeling approach is that we consider *cumulative* models for generation, export, and wastage, which allows us to define a conservation relationship linking these quantities to storage (Fig 2).

Let $G(t)$ denote the forecasted *cumulative* energy to be generated by the wind farm by the end of time step t. With usual notation, let $\Delta G(t) = G(t) - G(t-1)$ denote the forecasted *instantaneous* generation for time step t. Similarly let $E(t)$ denote the cumulative energy to be exported from the wind farm by the end of time step t and let $\Delta E(t) = E(t) - E(t-1)$. Let $b(t)$ denote the energy available in the battery at the end of time step t. Let B denote the battery capacity. Then $b(t)$ may be modeled recursively as follows:

$$b(t) = \min \ \{[b(t-1) + \Delta G(t) - \Delta E(t)]^+, \ B\} \tag{1}$$

If more energy is generated than exported at time step t, then $\Delta G(t) - \Delta E(t)$ is buffered in the battery provided this does not exceed the battery capacity. On the other hand, if more energy is exported than generated, $\Delta E(t) - \Delta G(t)$ is retrieved from the battery provided this is available. Since the energy stored in the battery is non-negative and can be at most B, the above equation follows.

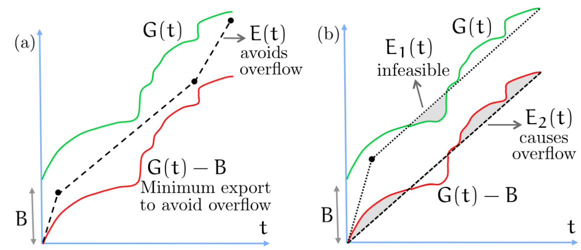

Fig. 3. Cumulative generation and export curves: (a) shows a piece-wise linear feasible export curve $E(t)$ that avoids overflow (b) shows two export curves. $E_1(t)$ is infeasible since it exports more than what is generated. $E_2(t)$ causes overflow since it does not export fast enough to avoid overflow.

Unfortunately Eq. (1) does not model the wastage of energy. The energy generated by the farm could be wasted due to the following reasons: (*i*) *Overflow* which occurs when the excess energy generated can neither be stored in battery nor exported for some reason. (*ii*) *Losses* which occur while charging or discharging the battery. Let $W(t)$ denote the cumulative energy to be wasted by the end of time step t. Now observe that, by the principle of conservation, the cumulative energy generated by the end of time step t must have been either exported, stored, or wasted. Therefore we have

$$G(t) = E(t) + b(t) + W(t) \tag{2}$$

With usual notation let $\Delta W(t) = W(t) - W(t-1)$ denote the energy wasted during time step t due to losses and overflow. Let $\omega \in (0, 1)$ denote the *loss factor* i.e. the fraction of energy lost while charging or discharging the battery. Thus we have

$$\Delta W(t) \geq \omega \ |b(t) - b(t-1)| = \omega \ |\Delta b(t)| \tag{3}$$

i.e. if energy is either stored or retrieved from the battery during a time step, a fraction of it is wasted. Additional wastage may result from overflow if there are constraints on export as well, as considered in the next section.

IV. Mitigating variability and maximizing export

We now consider the problem where the energy from a wind farm needs to be exported at a *uniform* rate based on a point forecast. Exporting at a uniform rate with a battery of finite capacity may result in wastage from overflow. Therefore we wish to maximize the amount of energy exported as well as minimize the variability i.e changes in the export rate. In other words, we seek a cumulative energy export curve $\{E(t)\}_t$ that is piece-wise linear with minimal discontinuities.

Fig. 3 shows the various cumulative curves. The curve $G(t)$ gives the (forecasted) cumulative energy generated by time step t. The curve $G(t) - B$ gives the minimum cumulative energy that must be exported by time t to avoid wastage by buffer overflow. Fig. 3(a) shows a feasible export curve that avoids buffer overflow. In Fig. 3(b), $E_1(t)$ is infeasible as in certain time steps, total energy exported is more than total generated (shown by shaded region). $E_2(t)$ causes overflow

$$
\begin{aligned}
&\text{Objective}: && \max_{\substack{E(t),W(t),b(t)\\ \forall t}} E(n)-\nu && (4)\\
&\text{Variation penalty}: && \nu=\gamma\sum_{t=1}^{n}|\Delta E(t)-\Delta E(t-1)| && (5)\\
&\text{Ramprate Limit}: && |\Delta E(t)-\Delta E(t-1)|\le r,\ \forall t && (6)\\
&\text{Conservation}: && G(t)=E(t)+b(t)+W(t)\quad \forall t && (7)\\
&\text{Cumulative}: && E(t)\ge E(t-1)\quad \forall t && (8)\\
& && W(t)\ge W(t-1)\quad \forall t &&\\
& && \Delta E(t)=E(t)-E(t-1)\quad \forall t &&\\
& && \Delta W(t)=W(t)-W(t-1)\quad \forall t &&\\
&\text{Battery}: && 0\le b(t)\le B\quad \forall t && (9)\\
&\text{Wastage}: && \Delta W(t)\ge \omega\ |b(t)-b(t-1)|\quad \forall t && (10)\\
&\text{Non negative}: && E(0)\ge 0,\quad W(0)\ge 0 && (11)\\
&\text{Input}: && G(t)\ \forall t,\ B,\ \gamma,\ \omega,\ r &&\\
&\text{Output}: && E(t),\ b(t),\ W(t)\ \forall t &&
\end{aligned}
$$

in certain time steps as the total energy exported is less than $G(t) - B$ (shown by shaded region). The above figure does not capture all the system constraints which are precisely expressed next using a mathematical program.

A. Mathematical Program

The linear program LP1:(4)-(11) yields a low variability cumulative export curve $\{E(t)\}_t$ given the forecast curve $\{G(t)\}_t$ for the next n time steps. The objective function in Eq. (4) maximizes the total energy exported and minimizes variability. The variability is measured using the variation penalty defined in Eq. (5) which measures the total rate change. A higher value of parameter γ decreases variability at the expense of reducing export while a lower value increases export at the expense of increasing variability. The parameter r in Eq. (6) is used to bound the individual rate changes in order to control the ramp-ups and dropoffs in the export. The battery, wastage, and conservation constraints are as modeled in the previous section. The cumulative constraints in Eq. (8) ensure that export and wastage are non-decreasing. The absolute value terms in the objective and constraints can be linearized using standard LP techniques.

B. Overflow Constraints: Mixed Integer Program

Observe that LP1 does not have any overflow constraints which ensure that energy is wasted only if it cannot be buffered in the battery. Thus LP1 is allowed to discard energy even if the battery is *not* full. This may be prevented by introducing the following integer binary constraints:

$$
\begin{aligned}
&\text{Overflow}: && \Delta W(t)-\omega|\Delta b(t)|\le M\ y(t)\ \forall t && (12)\\
& && b(t)\ge B\ y(t)\ \forall t &&\\
& && y(t)\in\{0,1\}\ \forall t &&
\end{aligned}
$$

Time step	Solution 1				Solution 2	
	$\Delta G(t)$	$\Delta E(t)$	$b_1(t)$	$\Delta W_1(t)$	$b_2(t)$	$\Delta W_2(t)$
i	10	10	0	0	0	0
$i+1$	30	10	18	2	18	2
$i+2$	20	10	20	8	18	10
$i+3$	15	10	20	5	20	3
$\vdots$	$\vdots$	$\vdots$	$\vdots$	$\vdots$	$\vdots$	$\vdots$

Fig. 4. Two different solutions with the same $\{E(t)\}_t$ but different $\{b(t)\}_t$ and $\{W(t)\}_t$. Capacity $B = 20$, the loss factor $\omega = 0.1$. In both cases the total energy wasted by the end of step $i+3$ is 15 units. Energy is buffered in step $i+2$ in solution 1 while in step $i+3$ in solution 2.

where M is a large constant, for instance, $M = \max_t \Delta G(t)$. These constraints ensure that whenever $\Delta W(t) - \omega|\Delta b(t)| > 0$, i.e. when there is an overflow, it must be the case that the battery is full, i.e. $b(t) = B$. Introducing overflow constraints into LP1 will yield a mixed integer program which we denote by MIP1:(4)-(12). Unfortunately MIPs are NP-hard and therefore computationally expensive, which can introduce challenges when delivering energy in real time. We now present an alternate approach that avoids these overflow constraints.

C. Linear solution processing

Lemma 1: Let f *denote the objective function* (4) *of* LP1 *and* MIP1. *Let* $X = (\{E(t)\}_t, \{b(t)\}_t, \{W(t)\}_t)$ *and* $X' = (\{E'(t)\}_t, \{b'(t)\}_t, \{W'(t)\}_t)$ *denote the optimal solutions of* LP1 *and* MIP1 *respectively for a given problem instance. Then* $f(X) = f(X')$, *although* $\{b(t)\}_t$ *and* $\{W(t)\}_t)$ *may be different from* $\{b'(t)\}_t$ *and* $\{W'(t)\}_t$.

The overflow constraints in MIP1 essentially ensure that energy is not wasted if it can be buffered and eventually exported. Although LP1 does not have these constraints, it cannot waste any exportable energy due to the following reasons. Observe that $W(t)$ is non-decreasing i.e. $W(t+1) \ge W(t)\ \forall t$. Thus if LP1 finds a solution that assigns $W(t_i) = x$, then for all subsequent time steps $t > t_i$, it must assign $W(t) \ge x$. This implies that any energy wasted during a time step is not available for use in subsequent time steps. Since the objective maximizes $E(n)$, LP1 can assign energy to $W(t)$'s only if that energy cannot be exported in subsequent steps by buffering. In fact LP1 can be regarded as a relaxation of MIP1, since the job of overflow constraints is partly handled by linear cumulative constraints on $W(t)$.

The consequence of this relaxation is that LP1 may have different solutions with the same export curve, which buffer earlier or later, but waste the same amount of energy eventually. An example of this is shown in Fig. 4, where two LP1 solutions $(\{E(t)\}_t, \{b_1(t)\}_t, \{W_1(t)\}_t)$ and $(\{E(t)\}_t, \{b_2(t)\}_t, \{W_2(t)\}_t)$ with the same export curve (hence the same objective value), waste energy at different time steps. Another example is when at the last time step $t = n$, keeping $E(n)$ fixed, one can move some energy from $b(n)$ to $W(n)$ without altering the objective value and obtain an alternate optimal solution to LP1. Thus a given $\{E(t)\}_t$ may have several feasible $\{W(t)\}_t$ and $\{b(t)\}_t$.

We now present a procedure to transform the optimal solution of LP1, $X = (\{E(t)\}_t, \{b(t)\}_t, \{W(t)\}_t)$ into an optimal solution of MIP1, $\overline{X} = (\{E(t)\}_t, \{\overline{b}(t)\}_t, \{\overline{W}(t)\}_t)$. Since the export curve and hence the objective value are unchanged, we have $f(\overline{X}) = f(X)$. The procedure is as follows:

---

function $\mathrm{transform}(\{b(t)\}_t,\ \{W(t)\}_t)$
for $t = 1$ to n **do**
  if $(\Delta W(t) > \omega|\Delta b(t)|)$ **then**
    $B' \leftarrow B - b(t)$ % available buffer space
    $B' \leftarrow \min\{\ B',\ (1-\omega)\Delta W(t)\ \}$
    $\overline{b}(t) \leftarrow b(t) + B'$ % move energy to buffer
    $\Delta\overline{W}(t) \leftarrow \Delta W(t) - B'$ % update wastage
  else
    $\overline{b}(t) \leftarrow b(t),\ \ \Delta\overline{W}(t) \leftarrow \Delta W(t)$
  end if
end for
return $(\{\overline{b}(t)\}_t,\ \{\overline{W}(t)\}_t)$

The $\mathrm{transform}$ procedure obtains $\{\overline{b}(t)\}_t$ and $\{\overline{W}(t)\}_t$ in $O(n)$ steps by moving any non-overflow energy in $\Delta W(t)$ to $\overline{b}(t)$, while taking losses into account. $\overline{X}$ still obeys all constraints of LP1 and also the overflow constraints of MIP1. Therefore $\overline{X}$ is a feasible solution of MIP1. Now we have $f(\overline{X}) = f(X) \geq f(X')$. The inequality follows since X satisfies only a subset of constraints satisfied by X'. Since X' is the optimal solution of MIP1, $f(X')$ is maximal and therefore $f(\overline{X}) = f(X')$. So $\overline{X}$ is also an optimal solution of MIP1.

Thus by omitting the overflow constraints, the optimal export curve $\{E(t)\}_t$ can be computed efficiently using LP1 in polynomial time. Additionally, $\{W(t)\}_t$ and $\{b(t)\}_t$ can be obtained using the fast $\mathrm{transform}$ procedure.

D. Uniqueness of export curve and other variation penalties

We now discuss if two different export curves $\{E_1(t)\}_t$ and $\{E_2(t)\}_t$ may both be optimal to LP1. To understand this, let vector $V = [\Delta E(2) - \Delta E(1), \ldots, \Delta E(n) - \Delta E(n-1)]$. The variation penalty $\nu = \gamma\|V\|_1$ (i.e. L_1 norm of V). Keeping $E(n)$ fixed, it is easy to see that one can construct vectors $V_1 \neq V_2$ such that $\|V_1\|_1 = \|V_2\|_1$ and both satisfy constraints of LP1. Therefore multiple export curves may yield the same objective function value (provided the ramprate limit r is sufficiently large). Fig. 5(a) shows an example of two export curves with the same objective value.

Since LP1 minimizes the L_1 norm of V, the vector V is expected to be sparse, i.e. the piece-wise linear export curve $\{E(t)\}_t$ has few discontinuities. An alternative variation penalty to consider is $\gamma\|V\|_2$ which yields a smooth export curve with several small linear segments. Using the L_2 norm for variation penalty in Eq. (5) results in a quadratic program that can still be solved using fast polynomial time algorithms.

E. Online extensions for real-time operation

LP1 determines a low variability energy export curve $\{E(t)\}_t$ given a forecast curve $\{G(t)\}_t$. Such an export curve can be used to deliver energy at a consistent rate in future. For instance given a day-ahead wind energy forecast, it can be used to compute a day-ahead low variability energy export curve. However during real-time operations, the forecast may

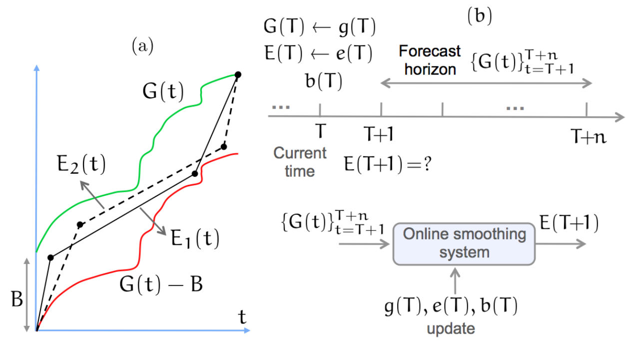

Fig. 5. ((a) Two different export curves $E_1(t)$ and $E_2(t)$ are shown which have the same variation penalty $\nu = \gamma\|V\|_1$ and objective value. (b) The online wind power smoothing system is shown which solves an optimization problem at each time step to determine the export rate at the next time step.

differ from actual generation and this needs to be considered in order to make decisions about future export. We now present an online wind power smoothing system that considers the actual energy generated so far, looks ahead at the forecast for the next n steps, and invokes LP1 in order to determine the energy to be exported during the next time step. The system repeats the process at each time step in a continuous manner (Fig. 5(b)).

Let $g(t)$ and $e(t)$ denote the actual cumulative energy generated and exported at the end of time step t respectively. Let the current time be the end of time step T, where the current battery state $b(T)$, the actual energy exported $e(T)$, and the actual generation $g(T)$ are known. The energy to be exported during the next time step, $E(T+1)$ is determined as follows:

---

function $\mathrm{online}(T)$
$(b(T), e(T), g(T)) \leftarrow \mathrm{system\_state}()$
$G(T) \leftarrow g(T),\ \ E(T) \leftarrow e(T)$
$W(T) \leftarrow G(T) - E(T) - b(T)$
$\{E(t), b(t), W(t)\}_{(T+1)}^{T+n} \leftarrow \mathrm{LP1}(\{G(t)\}_T^{T+n})$
return $\Delta E(T+1)$

Thus the online smoothing system instructs an energy delivery system to export $\Delta E(T+1)$ units of energy during time step $T+1$. The delivery system functions as follows:

---

if $\Delta g(T+1) > \Delta E(T+1)$ **then**
  store $\Delta g(T+1) - \Delta E(T+1)$ in buffer if possible
else
  retrieve $\Delta E(T+1) - \Delta g(T+1)$ from buffer if possible
end if

Thus wind power smoothing system repeats the function online again at the end of time step $T+1$.

F. Alternative variation penalty for micro-grids

In the case of micro-grids and captive power plants, wind power is complemented with non-wind generation to jointly serve loads locally. As the fraction of wind power increases, the load-following variability faced by non-wind generation increases as well, thus impacting its cost, efficiency, and reliability. We now show that LP1 can be extended to directly control the variability faced by non-wind generation.

Let $\ell(t)$ denote the total load jointly served by wind and non-wind generation. If $E(t)$ is the energy supplied by wind, then $\ell(t) - E(t)$ denotes the complementary energy supplied by non-wind generation. Although LP1 attempts to reduce the variability of wind energy $E(t)$, it can be extended to reduce the variability of the complementary energy supplied by non-wind generation. Given a cumulative load forecast $L(t)$, this is achieved by modifying LP1 as follows:

$$\text{Residual load:} \quad R(t) = L(t) - E(t) \tag{13}$$

$$\text{Variation penalty:} \quad \nu = \gamma \sum_{t=1}^{n} |\Delta R(t) - \Delta R(t-1)| \tag{14}$$

V. Mitigating variability and maximizing revenue

We now consider the problem where energy prices vary over time and we wish to determine an export curve $\{E(t)\}_t$ that maximizes revenue while minimizing variability. We consider a model where prices vary across time intervals and the variability within each interval needs to be minimized, i.e. the export curve will incur a rate-change penalty within a time interval but may change rates across time intervals.

Markets that determine energy prices are highly sophisticated and vary by location. However these are based on some common underlying principles that we consider in our work.

A. Day-ahead (DA) and Real-time (RT) Markets

Generators and retailers buy or sell energy in hourly DA and RT intra-hour markets. Both these are ex-*ante* markets, meaning that energy is actually delivered *after* the markets close and prices are set. The DA market is an hourly market while the RT market is generally for an interval within an hour (e.g. 15 min). DA markets generally close a day before while RT intra-hour markets close an hour or two before the actual intra-hour interval. RT balancing markets exist so that participants may bid their remaining resources based on a better forecast of grid conditions, demand, and supply. For e.g., a generator that has committed a certain amount of energy in DA market may participate as a consumer in the RT intra-hour market if she expects a shortfall of energy during a certain time interval. After the markets close, bids are evaluated and energy prices (also known as location-based marginal prices) are determined for the upcoming time interval. Thus each participant becomes committed for the delivery or consumption of a certain amount of energy at a specific price during an upcoming time interval. The DA and RT prices are generally different. Having gone through a two-settlement process to finalize commitments, if during actual operations, a generator delivers more or less than committed, she pays a penalty both for discarding as well as procuring the balance energy from ancillary or regulation services.

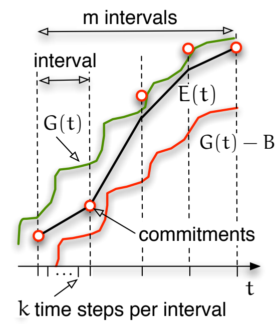

Fig. 6. Mitigating variability and maximizing revenue: A cumulative export curve $E(t)$ is shown along with the forecasted generation $G(t)$ and $G(t) - B$. The red circles show the energy commitments that have already been made through DA & RT markets and need to be met during each time interval. Since the energy prices vary across time intervals, the export curve attempts to maximize the total revenue earned by optimally meeting as many commitments as possible while minimizing the rate changes within each interval.

$$\text{Objective:} \quad \max_{\substack{E(t),W(t),b(t)\\ \forall t}} D - \sum_j \nu_j \tag{15}$$

Variation penalty for interval j:

$$\nu_j = \gamma' \sum_{t=(j-1)*k}^{j*k} |\Delta E(t) - \Delta E(t-1)| \quad \forall j = 1, \ldots, m \tag{16}$$

Energy supplied in jth interval:

$$e_j = E(j*k) - E((j-1)*k) \quad \forall j = 1, \ldots, m \tag{17}$$

Dollars for total energy supplied in m intervals:

$$D = \sum_{j=1}^{m} p_j^a c_j^a + p_j^r c_j^r - p_j^g |e_j - (c_j^a + c_j^r)| \tag{18}$$

Ramprate limit, Conservation, Cumulative, Battery, and Wastage constraints (6)-(11) of LP1 (19)

B. Mathematical program

We consider the above model wherein a wind power generator has firmed her supply commitments by successively bidding in DA and RT markets (based on the best available forecast and bid strategy). Having done that, during real time operations she is required to deliver her commitments within each intra-hour interval by exporting energy at a uniform rate. Let $j = 1$ denote the current intra-hour interval. We assume that markets have closed for all intervals $j = 1..m$. Let c_j^a and c_j^r denote the energy commitments to be met for jth interval from DA and RT markets respectively. Let $c_j = c_j^a + c_j^r$ denote the total energy commitment. Similarly let p_j^a and p_j^r denote the DA and RT market prices per unit of energy for the jth interval. Let p_j^g denote the price per unit of energy from regulation during the jth interval. Let e_j denote the total energy exported in the jth interval. Then the payment for this energy is $p_j^a c_j^a + p_j^r c_j^r - p_j^g |e_j - (c_j^a + c_j^r)|$ i.e., the payment for supplying the committed amount c_j after procuring or discarding the balance through regulation.

We consider a discrete time system as before with k time steps within each intra-hour interval. Let $n = k * m$ denote the total number of time steps across all m intervals and let $\{G(t)\}_t$ denote the forecast available for the n steps. Our goal is to determine the export curve $\{E(t)\}_{t=1}^{n}$ such that export rate changes are minimized within each interval and the total revenue is maximized (Fig. 6). Rate changes across intervals are not penalized. The linear program LP2:(15)-(19) achieves this objective and outputs an export curve for the next n time steps covering m intervals. Since LP2 looks ahead both at the forecast and energy commitments for the next m intervals, it optimizes across intervals to meet these commitments and maximizes revenue. The rate changes within intervals are penalized using the variation penalty (17) where γ' represents the cost of rate change. As in the case of LP1, LP2 is computationally efficient since the overflow constraints have been omitted. The optimality results of Lemma 1 continue to hold for LP2.

Similarly, the online smoothing system presented in IV-E can invoke LP2 instead of LP1 at each time step to export energy at a uniform rate to the grid. A variant of LP2 can also be used for planning purposes to participate in DA markets. For example, given the energy and DA price forecasts for 00-23 hours during the next day, LP2 can determine a low-variability energy export curve for the next day that maximizes revenue. This is achieved by replacing (18) by $D = \sum_j \widehat{p}_j e_j$, where $\widehat{p}_j$ denotes the forecasted energy price during each interval that now represents an hourly duration.

VI. Experiments

We conduct experiments using the historical wind energy data published by the Alberta Electric System Operator (AESO) [27]. AESO operates the Electric power system of Alberta, Canada and one of its primarily responsibilities is to economically and reliably dispatch generation to meet system load. AESO has published 10-min data about the total system load that it serves as well as the aggregate wind energy generation used in their system. The amount of wind energy in the system is not significant at the moment and varies from 0 to 8% (about 0.64GWh) of system load with an average of about 2.3%.

Figure 7(a) attempts to compare the variability of load with the variability of wind energy for a few days during the third quarter of 2011. The wind energy and load time series have both been normalized using their L_2 norms respectively in order to view them on the same scale. We observe that the system load exhibits a regular diurnal pattern and exhibits much lower variability than wind energy.

In order to estimate the operational impacts of injecting a large amount of wind energy into the system, we triple the amount of wind energy and subtract it off from the load to obtain the residual load that would be served by dispatching non-wind generation. Figure 7(b) plots the original system load along with the residual load. Wind energy now serves up to 24% of system load with an average of about 7%. We observe that the ramp range of system load is about 2GWh while the ramp range of residual load reaches 3GWh (annotated with arrow marks). When the wind generation is negatively correlated with the system load, it does not serve the peak load and therefore the residual load sometimes has the same peaks as the original load. However it reduces the minimum off-peak load thus increasing the ramp range of residual load. We also observe that residual load has thinner and sharper peaks as well as more short term variability compared to system load.

Increased ramp range implies that the system will be able to utilise less of cheap baseload generation (which is generally constant eg. coal, nuclear) and will need more of load following (e.g. hydro) and expensive & inefficient peaker generation (e.g. gas). Sharper peaks imply that the system needs more nimble generation that can ramp up and down rapidly. Increased short term variability implies that the system needs more regulation reserves to match the short term random fluctuations of load. All these factors can contribute to increasing the cost of non-wind generation as well as increase CO_2 emissions and may defeat the purpose of injecting wind generation into the system.

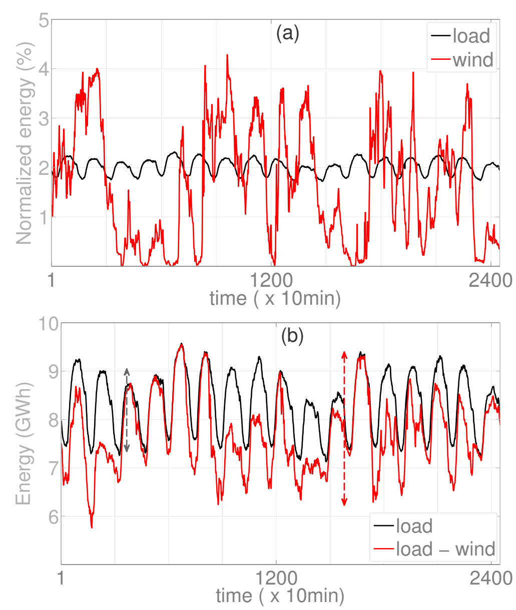

Fig. 7. (a) A comparison of variability of wind energy versus the variability of load. (b) Operational impacts of injecting wind energy: The original system load is shown along with the residual load (= load − wind) that needs to be served by non-wind generation.

Next we conduct Monte-Carlo simulations to study the smoothing behavior of LP1 that has been implemented using CPLEX [28]. We regard the daily 10-min wind generation time series as the forecasted generation curve $\{\Delta G(t)\}_t$ and use LP1 to compute the corresponding low-variability export curve $\{E(t)\}_t$ by varying over different storage sizes B and variation penalty factors γ while keeping the storage loss factor ω and ramp rate limit r fixed. We vary B in step sizes equal to the standard deviation of $\Delta G(t)$

Fig. 8(a) and (b) show the benchmark results using data for one of the sample days and plot the instantaneous and cumulative curves respectively. For this day, the wind generation sourced into the system varies between $135 - 585$ MWh. $\sigma(\Delta G(t)) \approx 96$ MWh. The blue curve in Fig. 8(a) shows the low variability export curve $\{\Delta E(t)\}_t$ when $B = \sigma(\Delta G(t))$ and $\gamma = 1$. Fig 8(b) shows the corresponding cumulative curve as a fraction of total energy generated. We observe that blue curve exports about 90% of the total wind energy generated.

Keeping B fixed, increasing γ yields the grey curve that has lower variability but also lower export as some of the energy is lost in overflow. Keeping γ fixed, increasing B yields the green curve that has higher export and also lower variability since γ also penalizes rate changes. The corresponding cumulative curves in Fig 8(b) show that the green curve has minimum variability and maximum export due to a large storage size.

Fig. 8(c) shows how the fraction of energy exported increases with buffer size for different γ. We observe that as γ increases, we need larger buffer sizes to export the same amount of energy. This is because as the variation penalty increases, the export curve becomes more smoother at the expense of potentially causing more overflow. For each value of variation penalty, at a certain point, the curve flattens out indicating that the system is exporting the maximum amount of energy. For instance, the blue curve which corresponds to the case when $\gamma = 1$, shows that it is sufficient to have a buffer $B = 2\sigma$ to export about 95% of energy. Thus the optimization framework could also be used to size batteries to achieve an acceptable level of smoothness and energy export with the help of historical wind energy data.

VII. Comparison with video smoothing problems

As mentioned earlier in section II, the wind smoothing problem has similarities with the video smoothing problem. The networking community has contributed a large body of literature on video smoothing, which covers different variants of this problem [21]–[26]. One of the basic variants is as follows. A streaming server wishes to transmit a stored VBR (variable bit rate) video to a client at a rate that has low variability. The client has a buffer of fixed capacity and attempts to play the video according to the video playback curve (which specifies the data required for each frame of video). The server is required to determine a piece-wise CBR (constant bit rate) export rate that has low variability and neither starves nor overflows the client buffer. Given a cumulative playback curve $G_v(t)$, a client buffer of size B_c, the server must transmit the video according to a cumulative export curve $E_v(t)$, such that the following holds at the client: $G_v(t) \leq E_v(t) \leq G_v(t) + B_c, \ \forall t$ (assuming a zero delay and loss network channel, see [21]). For the wind smoothing problem, given a forecasted generation curve $G(t)$ and a buffer of size B, the cumulative energy export curve $E(t)$ should be such that $G(t) - B \leq E(t) \leq G(t), \forall t$. However for a given video, the total amount of data to be transmitted is fixed and only the transmission variability needs to be minimized. In the problem addressed by LP1, both the total energy as well as variability are variables in optimization and one can transmit more or less energy depending on the cost of variability.

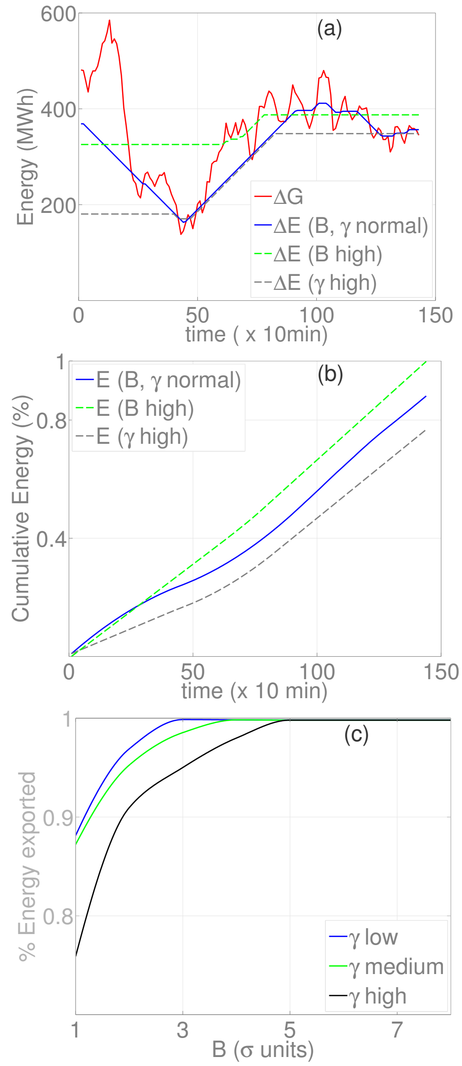

Fig. 8. Simulation results using daily 10-min historical wind energy data from AESO. (a, b): Instantaneous and cumulative export curves for different buffer sizes B and variation penalty γ, (c) Fraction of total energy exported as a function of buffer size B for different variation penalties γ.

Another important attribute of wind smoothing is the uncertainty of generation and the need for a forecast. The basic video variant above corresponds to stored video wherein the video playback curve is fixed and known. However one can formulate an equivalent problem in video streaming if the video is from a live event and is VBR. Let $G_{lv}(t)$ denote the cumulative forecasted video generation curve from a live event. Let B_s denote the buffer size at the server. Since B_s is constrained by the delay that can be introduced in live streaming, the buffer may overflow if the server does not transmit the video at the right rate. The server wishes to maximize export (or minimize losses) and minimize variability. The cumulative export curve $E_{l\nu}$ must be such that $G_{l\nu}(t) - B_s \leq E_{l\nu}(t) \leq G_{l\nu}(t), \forall t$. Therefore this problem is equivalent to the wind smoothing problem addressed in section IV and LP1 may be used to obtain an optimal solution. To the best of our knowledge, such a problem has not been addressed in the video literature. Another source of uncertainty in the video smoothing problem comes from the network channel that introduces delays and losses and this can modify the export curve seen at the client.

There are also a couple of system differences between video and wind problems. In the video problem, although the physical buffer is cheap, its size is constrained by the delay that it introduces. In the wind problem, the buffer size is limited by its price and can have charging/discharging losses. The wind problem also does not have any packet re-ordering issues which may arise in the video problem.

VIII. Conclusions and Discussions

Wind energy generation is expected to grow significantly over the next couple of years and therefore smoothing solutions to mitigate its variability are important to integrate it in a reliable and sustainable manner into power grids. In this work, we presented an optimization-based wind power smoothing system that uses storage to mitigate the variability of wind power. The system maximizes the energy exported or revenue earned. We presented a novel technique of modeling the buffer using only linear constraints that allows efficient computation of optimal smoothing solutions. Our work paves the way for computationally efficient smoothing systems that could be used in real-time operations.

We plan to extend our work in a couple of different directions. Future work will build upon the simulation experiments by considering forecast and generation together with different penalty metrics and battery sizes. We plan to extend our battery model to include varying loss rates, the number and depth of charging/discharging cycles, and battery lifetime. We plan to extend our optimization formulations to take into account stochastic forecasts by formulating stochastic linear programs that consider recourse models. Lastly, one of the challenges faced by wind farm operators is to optimally size the battery based on available wind conditions since battery storage systems are currently expensive. We shall study this problem in future.

References

[1] R. Katz, "Tech titans building boom," *Spectrum, IEEE*, vol. 46, no. 2, pp. 40 –54, Feb. 2009.

[2] R. Urgaonkar, B. Urgaonkar, M. J. Neely, and A. Sivasubramaniam, "Optimal power cost management using stored energy in data centers," in *Proceedings of the ACM SIGMETRICS*, 2011, pp. 221–232.

[3] K. Kusakana and H. J. Vermaak, "Hybrid renewable power systems for mobile telephony base stations in developing countries," *Renewable Energy*, vol. 51, pp. 419 – 425, Mar 2013.

[4] I. F. Bitterlin, "Modelling a reliable wind/pv/storage power system for remote radio base station sites without utility power," *Journal of Power Sources*, vol. 162, no. 2, pp. 906 – 912, 2006.

[5] "20% Wind Energy by 2030: Increasing Wind Energy Contribution to U.S. Electricity Supply, NREL report for US Dept. of Energy," 2008, www.nrel.gov/docs/fy08osti/41869.pdf.

[6] M. Ortega-Vazquez and D. Kirschen, "Estimating the spinning reserve requirements in systems with significant wind power generation penetration," *IEEE Transactions on Power Systems*, vol. 24, no. 1, pp. 114–124, Feb. 2009.

[7] B. Kirby and M. Milligan, "An examination of capacity and ramping impacts of wind energy on power systems," *The Electricity Journal*, vol. 21, no. 7, pp. 30–42, 2008.

[8] N. Kumar, P. Besuner, S. Lefton, D. Agan, and D. Hilleman, "Power Plant Cycling Costs," www.nrel.gov/docs/fy12osti/55433.pdf, Apr 2012, NREL report prepared by Intertek APTECH, Sunnyvale, California.

[9] E. Ela, M. Milligan, and B. Kirby, "Operating Reserves and Variable Generation," Aug. 2011, NREL Report No. TP-5500-51978.

[10] P. Denholm, E. Ela, B. Kirby, and M. Milligan, "The Role of Energy Storage with Renewable Electricity Generation," Jan. 2010, NREL Report No. NREL/TP-6A2-47187.

[11] E. Hirst, "Real-Time Balancing Operations and Markets: Key to Competitive Wholesale Electricity Markets (FERC Energy Policy)," 2001, wp.ornl.gov/sci/ees/etsd/pes/pubs/RTMReport.pdf.

[12] V. Arya and P. Dutta, "System and Method for Smoothing Power from Wind Farms," Patent Pending US 13/441235, April 2012.

[13] C. Monteiro, R. Bessa, V. Miranda, A. Botterud, J. Wang, and G. Conzelmann, "Wind power forecasting: State of the art," in *ANL/DIS-10-2, Argonne National Laboratory, USA*, 2009.

[14] "ARMINES Wind Power Prediction System," http://www.scep.ensmp.fr/prediction/.

[15] "ENFOR Wind Power Prediction Tool," http://www.enfor.eu/wind_power_prediction_tool_wppt.php.

[16] H. Chen, T. N. Cong, W. Yang, C. Tan, Y. Li, and Y. Ding, "Progress in electrical energy storage system: A critical review," *Progress in Natural Science*, vol. 19, no. 3, pp. 291 – 312, 2009.

[17] J. Barton and D. Infield, "Energy storage and its use with intermittent renewable energy," *IEEE Transactions on Energy Conversion*, vol. 19, no. 2, pp. 441–448, 2004.

[18] S. Teleke, M. Baran, A. Huang, S. Bhattacharya, and L. Anderson, "Control strategies for battery energy storage for wind farm dispatching," *IEEE Transactions on Energy Conversion*, vol. 24, no. 3, pp. 725–732, Sept. 2009.

[19] X. Wang, D. Mahinda Vilathgamuwa, and S. Choi, "Determination of battery storage capacity in energy buffer for wind farm," *IEEE Transactions on Energy Conversion*, vol. 23, no. 3, pp. 868–878, Sept. 2008.

[20] A. Arulampalam, M. Barnes, N. Jenkins, and J. Ekanayake, "Power quality and stability improvement of a wind farm using statcom supported with hybrid battery energy storage," *IEE Proceedings on Generation, Transmission and Distribution*, vol. 153, no. 6, pp. 701–710, Nov 2006.

[21] J. D. Salehi, Z.-L. Zhang, J. F. Kurose, and D. F. Towsley, "Supporting stored video reducing rate variability and end-to-end resource requirements through optimal smoothing," *IEEE/ACM Trans. Netw.*, vol. 6, no. 4, pp. 397–410, 1998.

[22] S. S. Lam, S. Chow, and D. K. Y. Yau, "An algorithm for lossless smoothing of MPEG video," *ACM SIGCOMM Comput. Commun. Rev.*, vol. 24, no. 4, pp. 281–293, 1994.

[23] T. Ott, T. V. Lakshman, and A. Tabatabai, "A scheme for smoothing delay-sensitive traffic offered to ATM networks," in *INFOCOM*, 1992, pp. 776 –785 vol.2.

[24] N. B. Shroff and M. Schwartz, "Video modeling within networks using deterministic smoothing at the source," in *INFOCOM*, 1994, pp. 342 –349 vol.1.

[25] S. Sen, J. Dey, J. Kurose, J. Stankovic, and D. Towsley, "Streaming CBR transmission of VBR stored video," in *SPIE Symposium on Voice Video and Data Communications*, 1997.

[26] P. Dutta, A. Seetharam, V. Arya, M. Chetlur, S. Kalyanaraman, and J. Kurose, "On managing quality of experience of multiple video streams in wireless networks," in *INFOCOM*, 2012, pp. 1242 –1250.

[27] "Alberta Electric System Operator (AESO)," http://www.aeso.ca/gridoperations/20544.html.

[28] IBM ILOG, "CPLEX: High-performance software for Mathematical Programming and Optimization."